Scripta Materialia 113 (2016) 10–13

Contents lists available at ScienceDirect

Scripta Materialia

journal homepage: www.elsevier.com/locate/smm

Toughen and harden metallic glass through designing statistical heterogeneity

Yongwei Wang [a,c], Mo Li [b,c,*], Jinwu Xu [a]

[a] School of Mechanical Engineering, University of Science and Technology Beijing, Beijing 100083, China
[b] State Key Laboratory of Advanced Metallic Materials, University of Science and Technology Beijing, Beijing 100083, China
[c] School of Materials Science and Engineering, Georgia Institute of Technology, Atlanta, GA 30332, United States

ARTICLE INFO

Article history:
Received 25 August 2015
Received in revised form 20 September 2015
Accepted 20 September 2015
Available online 24 October 2015

Keywords:
Metallic glass
Mechanical properties
Toughness
Work hardening

ABSTRACT

Although having remarkable mechanical properties, metallic glass is severely limited by the lack of toughness and hardening ability which are among the basic requirements for structural and functional applications. Various attempts have been made experimentally to address these issues but with very limited improvement. Here we report a new attempt via material design approach using finite element modeling. We deliberately introduce statistical heterogeneity into the metallic glass samples, i.e. free volume dispersity. We show that the plasticity and toughness can be enhanced systematically with the increase of the heterogeneity and in certain circumstance even apparent hardening can be achieved. We will discuss the underlying mechanisms and also possible design of new metallic glass composites using the concept of heterogeneity dispersion.

Metallic glass (MG) is a structurally disordered alloy without the long-range periodic atomic order. The atomic packing makes the MG free of the structural defects and microstructures such as dislocations and grain boundaries, both of which are commonly seen in crystals. The lack of the structural feature gives rise to some remarkable mechanical properties, such as high strength and large elastic limit as compared to its crystalline counterparts, but at the same time, some of the disabling shortcomings for structural and functional applications. The foremost is the lack of plasticity and associated toughness. For example, under unconstrained deformation mode such as tension, there is little plastic deformation. Therefore, MG in general appears brittle or has low toughness, although a small number of systems exhibit incredible toughness [1,2]. The brittleness is originated primarily from a deformation mechanism called shear localization (SL): when the yield point is reached, metallic glass deforms plastically in narrow regions called shear bands (SBs). Usually one or a few bands develop and carry all plastic strain, making the sample break in brittle manor. Therefore, the natural strategy to toughen MG is to enhance plasticity, specifically by controlling shear banding. This has been done almost exclusively so far by putting different types of inclusions into the glassy matrix [3–10]. Both soft and hard crystalline phases have been tried and recently certain specific phases with extended deformability such as Martensites are used as well [11–14]. The heterogeneous phases act as a barrier to shear band formation and propagation. Although in some cases extended plasticity or toughness has been achieved, the desired hardening as well as tensile ductility has not been obtained for all systems.

The underlying mechanism of strain localization is related to changes in local atomic packing, primarily the open space around atoms, or free volumes (FVs) [15,16]. The more free volumes there are either initially present in the sample or through subsequent deformation, the softer the metallic glass is and more prone to develop SL. Harder or stronger inclusions can certainly block or alter the SB propagation as seen in some composites and sometimes change shear banding initiation [1–14]. But the presence of the heterogeneous phase with the MG matrix causes stress concentration and incompatibility in deformation strain, that can and often leads to detrimental result to the overall mechanical properties. Moreover, since it is difficult to control the inclusions, i.e. their size, shape and dispersity, the improvement in gaining toughness is often circumstantial and marginal. Therefore, to date little is known about the *design limit* of the mechanical performance of MG and its composites.

Since the major cause for failure in MG and composites is related to deformation incompatibility, if these effects could be alleviated or rectified, better MGs and composites could be made. This can be realized through designing dispersity of free volumes. Two types of design parameters are relevant: (1) the size, shape, and density of the different glassy regions and (2) the magnitude or concentration of free volumes inside these regions. The former is related to the *spatial heterogeneity*, and the latter the *material* information, which as shown below can be manipulated through statistical methods. There are two scenarios for the design ideas, one is the conventional crystal-in-glass composite

* Corresponding author at: School of Materials Science and Engineering, Georgia Institute of Technology, Atlanta, GA 30332, United States.
E-mail address: mo.li@gatech.edu (M. Li).

http://dx.doi.org/10.1016/j.scriptamat.2015.09.038
1359-6462/

and the second is the "*glass-in-glass*" system, monolithic or composite. In the former, abrupt structural and compositional change occurs across the amorphous-crystal interface and the different deformation behaviors of the two phases exist and in the latter these properties can be tuned and may be effectively controlled. For example, the free volume concentration inside each region can vary smoothly while the overall structure of the sample is kept amorphous. We call it *statistical heterogeneity*. In this paper we shall focus on this route and its consequence in improving mechanical properties in MG and possibly its composites. We show that with the increase of the statistical heterogeneity, the plasticity and toughness can be enhanced systematically and in certain circumstances, even "work hardening" can be achieved.

The idea is carried out by two steps. The first is to generate the statistical heterogeneity and the second to perform deformation simulation to measure the corresponding mechanical properties. The test samples are prepared by assigning free volumes, $v(r)$, at specific location r in a sample. As mentioned above, we can vary $v(r)$ either spatially to generate certain patterns or statistically by focusing on a specific spatial pattern but with free volumes with different variance and magnitude. Here we shall limit ourselves to the latter for simplicity in illuminating the concept, while the former will be presented in a separate publication.

Specifically, for a given spatial FV distribution we vary the magnitude and variance of the free volumes $v(r)$ drawn from a certain statistical distribution $P(v)$. Often randomly dispersed free volumes following a Gaussian distribution are considered for MGs [17–19]. In this work, a more general approach is considered. There are two statistical parameters that one can manipulate, the mean and variance of the free volumes. We have learned that the variance or dispersity seems to have unusual power in leveraging the plasticity of metallic glasses. For this reason, we designed a series of samples with different variances of free volume.

To systematically produce the variance and compare the results, we chose to use beta distribution function. There are two additional reasons: Firstly, unlike Gaussian, beta distribution has finite cut-off, so it is easy to model the FVs because in real samples the FVs are bounded from above and below. Secondly, the variance can be made symmetric (or asymmetric) which is easy for characterizing the results. In this work, all samples are produced with the free volume obtained via the transformation relation $0.04Beta(a, b) + 0.03$ with a and b being the two parameters characterizing the *Beta* distribution with a different standard deviation (see Table 1). The range of the free volumes is limited from 0.03 to 0.07 with the mean at 0.05; the variance is changed by varying a and b.

The mechanical properties are obtained by using a finite element modeling. In this work, we use an elasto-plastic constitutive model modified to incorporate explicitly the free volume variation in metallic glass. The technical details can be found in Refs. 17–19. Here we give only a brief description. First, the deformation is decomposed into elastic and plastic part, $\varepsilon_{ij} = \varepsilon_{ij}^{el} + \varepsilon_{ij}^{pl}$, where ε_{ij}^{el} is the elastic strain of an isotropic sample and $d\varepsilon_{ij}^{pl} = d\lambda \frac{\partial g}{\partial \sigma_{ij}}$ the plastic flow equation for the plastic potential function $g(\sigma_{ij}) = b'I_1 + \sqrt{3J_2} - K$ from the Drucker–Prager (DP) type of yield surface function, λ the plastic deformation parameter related to free volume change, σ_{ij} the Cauchy stress, and I_1 the first invariant of σ_{ij} and J_2 the second invariant of the deviatoric stress. The effective stress and strain are $\sigma_{DP} = a'I_1 + \sqrt{3J_2}$ and $d\varepsilon_{eff}^{pl} = \sqrt{2/3 d\varepsilon_{ij}^{pl} d\varepsilon_{ij}^{pl}}$. a', b' and K are constant; and we have $a' = b'$, or associated flow rule in this work.

The plastic strain parameter is connected to the free volume production [19,20] via $\dot{\varepsilon}_{eff}^{pl} = 2f \exp(-\alpha v^*/\bar{v}_f) \exp(-\frac{\Delta G^m}{k_B T}) \sinh(\frac{\tau\Omega}{2k_B T})$ and $\frac{\partial \bar{v}_f}{\partial t} = v^* f \exp(-\alpha v^*/\bar{v}_f) \exp(-\frac{\Delta G^m}{k_B T})[\frac{2\alpha k_B T}{\bar{v}_f S}(\cosh(\frac{\tau\Omega}{2\alpha k_B T}) - 1) - \frac{1}{n_D} + \kappa \nabla^2 \bar{v}_f]$, where $\bar{v}_f$ is the mean free volume, α a geometrical factor close to 1, v^* the hard-sphere volume of atom, k_B the Boltzmann constant, Ω the atomic volume, τ the shear stress, ΔG^m the activation energy, f the frequency of atomic vibration, T temperature, n_D the number of atomic jumps needed to annihilate a free volume equal to v^* which ranges between 3 and 10, and $S = \frac{E}{3(1-\mu)}$, where E is the Young's modulus and μ Poisson ratio, and κ the free volume gradient coefficient.

We solve the above nonlinear equations for $\bar{v}_f$ and ε_{ij}. The material tangent $D_{ijkl}^{ep} = \partial \Delta\sigma_{ij} / \partial \Delta\varepsilon_{kl}$ is implemented in ABAQUS finite element software through a UMAT subroutine. We use bulk metallic glass $Zr_{41.25}Ti_{13.75}Ni_{10}Cu_{12.5}Be_{22.5}$ as an example and the related material parameters can be found in Ref. 19. The samples are kept at 300 K and have the periodic boundary conditions and 7500 regular mesh elements. Plane strain tension and compression load are applied to the samples with the strain rate of 0.1/s. In the following we shall present the results on a typical case with the FV bounded in the range between 0.03 and 0.07 around the mean at 0.05. The variance or statistical heterogeneity is selected by varying a and b (see Table 1).

The tensile stress–strain relations are shown in Fig. 1. For case A which has the smallest standard deviation at 0.002 around the mean, the stress–strain relation follows that typical for metallic glasses [17–20]: an elastic regime before yielding which is marked by the deviation from the linear elastic behavior using the 0.2% off-set method, and when the stress reaches the maximum value, a precipitous drop follows. The rapid stress decline within a short strain range indicates brittleness of the sample. Since the periodic boundary conditions are used, the sample cannot be sheared off and thus the stress does not drop to zero as often seen in experiment. As the variance increases further, we observe that the strain range in which the peak stress drops to a stable value becomes further extended. For example, for case B with a standard deviation of 0.006, the strain range is 5.3% larger. However, the peak stress and the yield stress get smaller, which suggests that the gaining in plasticity is at the cost of the strength for the glass-in-glass model.

Note that the free volume dispersion in cases A and B follows the distribution resembling closely a truncated Gaussian [21]. Further, we realize that by simply increasing the variance if the distribution remains

Table 1
The standard deviation (SD) of the free volumes and the corresponding parameter a and b used in symmetric (A to E) and asymmetric (F and G) beta distribution.

System	a	b	SD, 10^{-3}	Mean
A	50	50	2.0	0.05
B	5	5	6.0	0.05
C	1	1	11.5	0.05
D	0.5	0.5	14.2	0.05
E	0.1	0.1	18.3	0.05
F	5	7	5.5	0.0483
G	7	5	5.5	0.0517

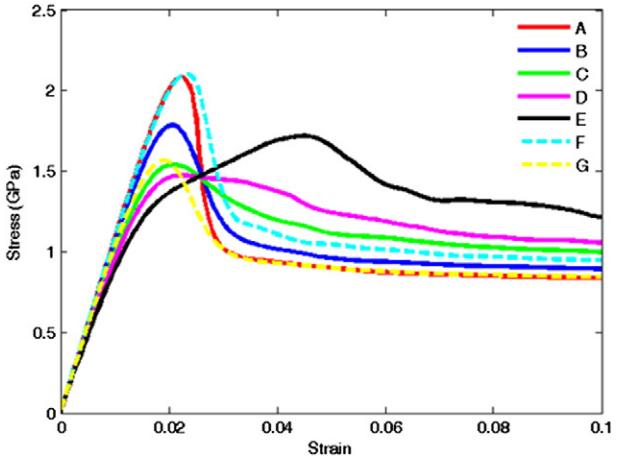

Fig. 1. The tensile stress–strain relations versus the applied strain in the samples from Table 1.

Gaussian-like, the stress–strain relation remains qualitatively the same as shown in cases A and B. At the extreme case C where the free volume follows a random uniform distribution, the stress–strain relation behaves qualitatively the same as in case A and B.

To break this trend, a different distribution and dispersion of free volume must be considered, which leads us to cases D and E where the variance is enlarged while the mean remains the same. Specifically, we chose the free volume that follows the symmetric beta distribution. The free volumes generated have two peaks, one with high and another with low free volume. This strategy results in a fundamentally different result. The stress–strain curve in Fig. 1 shows that when we disperse the free volumes on the mesh points with increasing dispersity, the stress–strain curve becomes stabilized, that is, the sudden stress drop from the maximum value disappears in case D; and even starts to recover from the drop and rises up again in case E. This dramatic turnaround as the function of the free volume dispersity indicates not only the improved plasticity but also strengthening and even "hardening".

The strength is measured by the yield stress σ_{yield} and the peak stress $\sigma_{\max}$ which can be easily obtained from the stress–strain curves. The plastic strain needs to be defined specifically here. As the failure strain in the modeling is finite, we define this strain as that corresponding to the falling stress $\sigma_{failure}$ after it reaches the maximum value $\sigma_{\max}$. Specifically, $\sigma_{failure} = \frac{1}{2}(\sigma_{\max} + \sigma_{steady})$, where σ_{steady} is the steady stress when the stress falls to (experimentally it is often zero as the sample shears off). The failure strain $\varepsilon_{failure}$ corresponding to $\sigma_{failure}$ can thus be located. Using $\varepsilon_{failure}$, we can define a measure of plasticity between $\varepsilon_{failure}$ and the yield strain ε_{yield} corresponding to the yield stress σ_{yield}, $\Delta\varepsilon = \varepsilon_{failure} - \varepsilon_{yield}$. Obviously, the larger $\Delta\varepsilon$ is, the larger the total plasticity. Another measure takes into account the difference in the stress drops, $\Delta\sigma_{drop} = \sigma_{\max} - \sigma_{failure}$ and the corresponding strain change, $\Delta\varepsilon_{drop} = (\varepsilon_{\max} - \varepsilon_{failure})$, that is, $\beta = \Delta\varepsilon_{drop}/(\frac{\Delta\sigma_{drop}}{\sigma_{failure}})$. β is actually the failure strain range when the system stress drops from the maximum to the failure stress weighted by the stress drop. It thus measures the elongation per stress drop, or the "surviving" plastic strain when failure occurs. Obviously the smaller $\Delta\sigma_{drop}$ and/or larger $\Delta\varepsilon_{drop}$ is, the larger β, and the larger the plasticity. Clearly, β is applicable only for cases A to D but not for case E where $\Delta\sigma_{drop}$ is not well defined; but $\Delta\varepsilon$ is applicable for all cases.

In Fig. 2 we summarize the change of the plastic strain as well as strength in different samples. For cases A to C, an increase in the variance clearly leads to improvement of plasticity but marginal, as shown by both $\Delta\varepsilon$ and β; and the increase in the plasticity is compensated by the loss of strength. However, for cases D and E, the plastic strain measured by $\Delta\varepsilon$ increases dramatically; in addition, the peak stress in case E increases, indicating not only toughening but also "work hardening" ability.

The shift in the mechanical behaviors is originated from the different dispersity of free volume. Cases D and E practically follow *bimodal dispersion* where the large free volumes are intermixed randomly with the small ones. The mesh points with large free volumes are softer and thus deform easily, while those with small ones are more rigid and would show delay in deformation. When mixed, they contribute to plasticity and strength in complex and yet predictable ways: (1) the softer parts deform at low stress and contribute a large part to plasticity, (2) the rigid parts contribute to plasticity also, but mainly through blocking the local shear deformation initiated in the softer region first and later on the shear band propagation in itself, and (3) the rigid parts also contribute to strengthening the system through the rule of mixing, which is manifested as the rise of the peak stress or apparent "work hardening".

The above mechanism is captured unambiguously from the evolution of the local strain and free volume from the two extreme examples for the brittle to ductile change, cases A and E. They show very different local strain (Figs. 3 and 4 (a)–(d)) and free volume and (Figs. 3 and 4 (e)–(h)). For Case A, the local deformation initiates at the soft mesh points and is distributed uniformly in early stage deformation

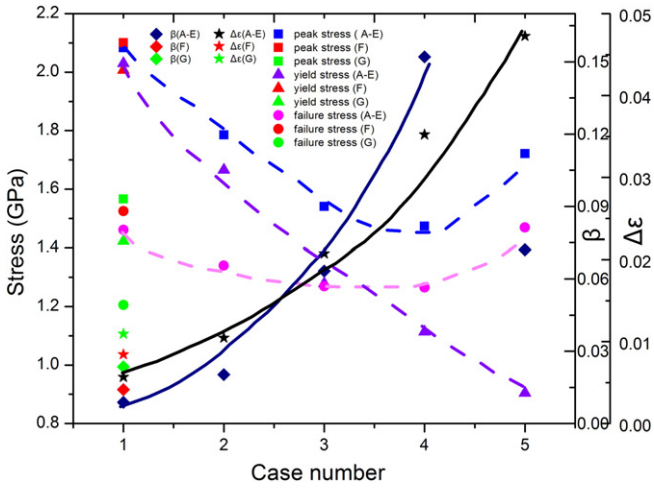

Fig. 2. The peak stress, yield stress, and plastic strain in different cases with the corresponding free volume dispersity. The number of case labeled as 1 to 5 corresponds to cases A to E. Two cases, F and G, with asymmetric free volumes are also shown. The lines are the guide for the eyes.

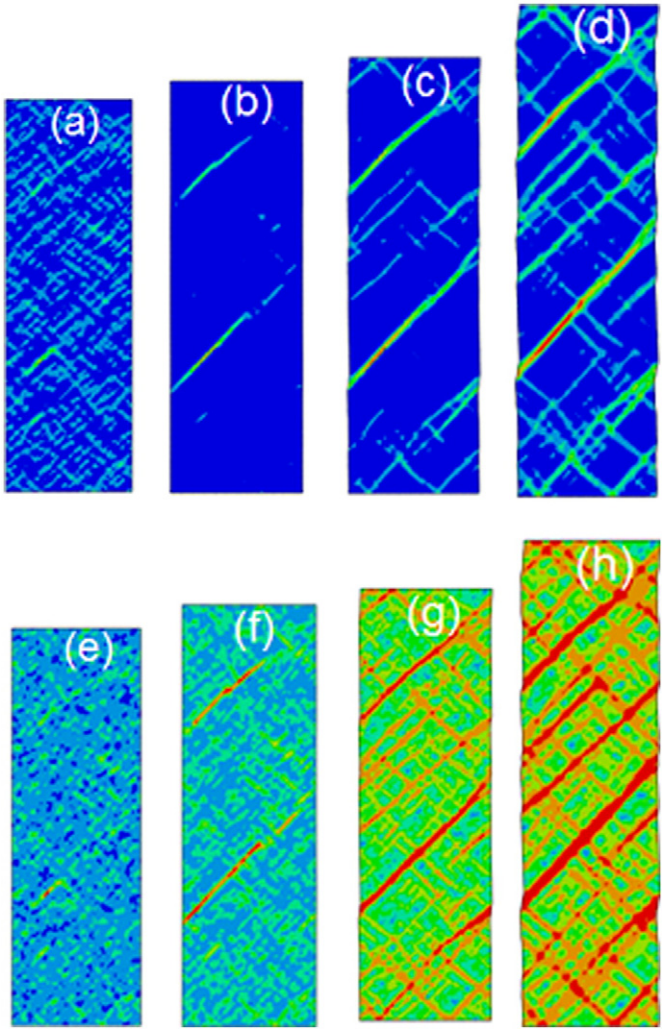

Fig. 3. The local strain (a to d) and free volume (e to h) distribution in the brittle sample A at different applied external tensile strains: (a & e) 0.024, (b & f) 0.025, (c & g) 0.050, and (d & h) 0.10. The color scheme is arbitrary to reflect the best visual effect: the warmer the color, the higher the local strain and volume.

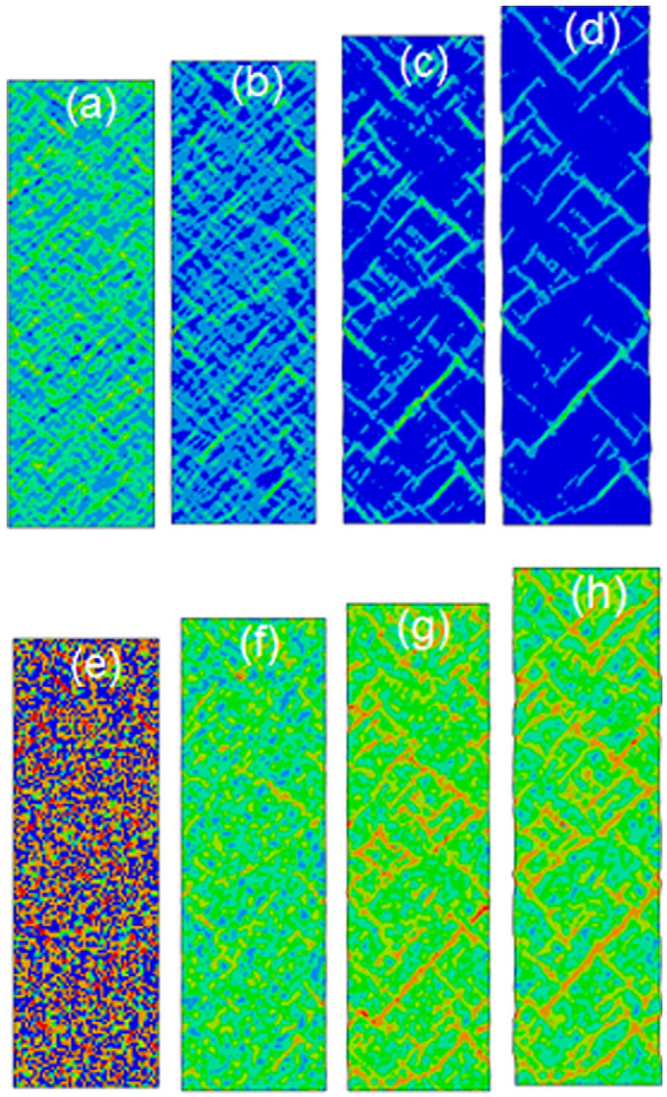

Fig. 4. The local strain (a to d) and free volume (e to h) distribution in the ductile sample E at different applied external tensile strains: (a & e) 0.018, (b & f) 0.040, (c & g) 0.067, and (d & h) 0.10. The color scheme is arbitrary to reflect the best visual effect: the warmer the color, the higher the local strain and volume.

(Fig. 3(a) and (e)); and as the deformation continues, the local strain regions become extended to include other nearby mesh point regions and then connected at larger deformation (Fig. 3(b) and (c) and (f) and (g)) and eventually localized at large strain (Fig. 3(d) and (h)). The sample has many localized deformation zones including the ones causing the final failure.

In contract, in the ductile case E, initial deformation started at the soft mesh points continues to be localized around their original location (Fig. 4(a) and (e)); and as the deformation continues, the deformation regions are still restricted to their original location although more new deformed regions are created elsewhere including those with larger free volumes (Fig. 4(b) and (c) and (f) and (g)). When localized regions have finally developed, the deformation bands do not look smooth and straight as in Case A, rather rugged and zigzag with many side bands (Fig. 4(d) and (h)). Contrast to case A, the localized deformation zones are spread more widely and no through shear band across the sample forms at larger deformation. When finally the hard regions begin to deform at large deformation, the new and the already-deformed regions become intertwined, leading to the apparent "hardening" effect seen in the stress–strain curves.

In summary, we have systematically investigated the possibilities of making tough and strong metallic glasses. By exploiting the statistical heterogeneity or dispersity of free volume, we are able to see clearly the variation of free volume and its effects on plasticity. While the mean free volume does little to change the plasticity (see the asymmetric distribution and its effects in Figs. 1 and 2), when changed from that of Gaussian-like to bimodal distribution with increasing dispersity, the metallic glasses start to exhibit a fundamental shift in their mechanical behaviors: the material can be toughened and even "hardened" if proper heterogeneity is introduced. The mechanism is the combined contribution from the softer and harder regions — the soft region contribute to plasticity and so is the harder region which is manifested primarily through blocking the localized deformation in the soft regions. At larger deformation, the hard region starts to deform and contributes to strengthening and when the deformation in the soft and hard regions begin to interact strongly, "hardening" can be achieved.

The mechanism revealed from computation modeling suggests a viable route to toughen metallic glass by introducing heterogeneity free of structural discontinuity, the "glass-in-glass" composite made of hard and soft metallic glasses. However, in making this new MG composite, one must face other issues both practical and basic to design and understanding of these materials. One is the *relevant length scale*. In this work, the heterogeneity is only limited to the mesh size. What happens if we introduce spatial variations or heterogeneities? And is there an optimal size of the heterogeneity that could allow us to obtain the maximum strength and toughness? The second is the structure and mechanical properties of the interfacial regions between the heterogeneities. Clearly, the mechanical properties and shape and size of interfaces are crucial to the overall mechanical response of MG composites, which is the motivation behind the recent exploitation of the interface in the so-called nanoglass [21,22]. Finally, thermal diffusion assisted annihilation reduces the effectiveness of the FV heterogeneity. How high this temperature limit is needs to be studied. We shall address these issues subsequently.

Acknowledgment

The work is supported by the National Thousand Talents Program of China.

References

[1] M.D. Demetriou, M.E. Launey, G. Garrett, G.P. Schramm, D.C. Hofmann, R.O. Ritchie, Nature Mater. 10 (2011) 123–128.
[2] Q. He, J.K. Shang, E. Ma, J. Xu, Acta Mater. 60 (2012) 4940–4949.
[3] H. Choi-Yima, W. L. Johnson. Appl. Phys. Lett. 71 (1997) 3808–3810.
[4] R.D. Conner, R.B. Dandliker, W.L. Johnson, Acta mater. 46 (1998) 6089–6102.
[5] C.P. Kim, R. Busch, A. Masuhr, H. Choi-Yim, W. L. Johnson. Appl. Phys. Lett. 79 (2001) 1456–1458.
[6] D.C. Hofmann, J.Y. Suh, A. Wiest, G. Duan, M.L. Lind, M.D. Demetriou, W.L. Johnson, Nature 451 (2008) 1085–1089.
[7] C.C. Hays, C.P. Kim, W. L. Johnson. Phys. Rev. Lett. 84 (2000) 2901–2904.
[8] H.F. Zhang, H. Li, A.M. Wang, H.M. Fu, B.Z. Ding, Z.Q. Hu, Intermetallics 17 (2009) 1070–1077.
[9] J. Das, M.B. Tang, K.B. Kim, R. Theissmann, F. Baier, W.H. Wang, Jurgen Eckert. Phys. Rev. Lett. 94 (2005) 205501.
[10] D.C. Hofmann, Journal of Materials 2013 (2013) 1–8.
[11] Y.F. Sun, B.C. Wei, Y.R. Wang, W.H. Li, T.L. Cheung, C.H. Shek, Appl. Phys. Lett. 87 (2005) 051905.
[12] S. Pauly, J. Das, a J. Bednarcik, N. Mattern, K.B. Kim, D.H. Kimd and J. Eckert, Scripta Mat. 60 (2009) 431–434.
[13] Y. Wu, D.Q. Zhou, W.L. Song, H. Wang, Z.Y. Zhang, D. Ma, X.L. Wang, Z.P. Lu, Phys. Rev. Lett. 109 (2012) 245506.
[14] D.C. Hofmann, Science 329 (2010) 1294–1295.
[15] F. Spaepen, Acta Mat. 25 (1977) 407–415.
[16] A. Argon, Acta Mat. 27 (1979).
[17] Y.F. Gao, Modelling Simul. Mater. Sci. Eng. 14 (2006) 1329–1345.
[18] J. Mater, Res. 24 (2009) 2688–2696.
[19] M. Zhao, M. Li, Metals 2 (2012) 488–507.
[20] M. Zhao, M. Li. Appl. Phys. Lett. 93 (2008) 241906.
[21] J. Jing, A. Kramer, R. Birringer, H. Gleiter, U. Gonser, J. Non-Cryst. Solids 113 (1989) 167.
[22] H. Gleiter, Beilstein J. Nanotechnol. 4 (2013) 517.